Hyperfine Interactions **139/140:** 33–40, 2002.

Iron Uniform-Size Nanoparticles Dispersed on MCM-41 Used as Hydrocarbon Synthesis Catalyst

S. G. MARCHETTI[1,2], M. V. CAGNOLI[1,2], A. M. ALVAREZ[1,2], J. F. BENGOA[1], N. G. GALLEGOS[1,3], A. A. YERAMIÁN[1,2] and R. C. MERCADER[4]

[1] *Centro de Investigación y Desarrollo en Procesos Catalíticos (CINDECA, CONICET, CIC), Universidad Nacional de La Plata, 47 115, 1900 La Plata, Argentina*
[2] *Departamento de Química, Facultad de Ciencias Exactas, Universidad Nacional de La Plata, 47 115, 1900 La Plata, Argentina*
[3] *Departamento de Química, Facultad de Ingeniería, Universidad Nacional de La Plata, 47 115, 1900 La Plata, Argentina*
[4] *Departamento de Física, IFLP, Facultad de Ciencias Exactas, Universidad Nacional de La Plata, 47 115, 1900 La Plata, Argentina*

Abstract. We have synthesized mesoporous MCM-41 and have used it as a support for iron particles to be employed as a catalyst in the Fischer–Tropsch reaction. The solids were characterized by Mössbauer spectroscopy, X-ray diffraction, BET, TGA, CO chemisorption and volumetric oxidation. Although the catalyst showed a high CO conversion when it was used in the hydrocarbon synthesis from CO and H_2 (14.3% at 1 h of reaction time) mainly methane was formed. The high methane production is likely related to the very small size of the metal particles obtained. We suggest some ways to improve the selectivity.

Key words: mesoporous material, Fischer–Tropsch reaction, Fe/MCM-41, nanoparticles.

1. Introduction

MCM-41 belongs to the M41S mesoporous molecular sieve family, with a hexagonal arrangement of uniform channels of 15–100 Å diameters. Because of its very high surface area and its narrow size pore distribution [1], MCM-41 seems to be a good support material for iron metallic particles to be used in hydrocarbon synthesis. To this end, we have prepared MCM-41 and have been able to disperse very small iron particles inside the channels of the mesoporous solid. In this work, we report the materials characterization and the activity and selectivity tests carried out on the resulting catalyst for CO hydrogenation reaction.

2. Experimental section

We have synthesized MCM-41 following one of Beck's recipes [1]; 40.0 g of water, 20.6 g of sodium silicate (26.1% silica), and 1.2 g of sulfuric acid combined with

stirring. After allowing the resulting mixture to stir for 10 minutes, the surfactant template solution (16.8 g of cetyl-trimethyl-ammonium bromide + 50.2 g of water) was added, and the resulting gel was stirred for 0.5 h; 20.0 g of water were then added to the gel. This was heated at 373 K for 144 h in a static autoclave. After cooling to room temperature (RT), the resulting solid product was recovered by filtration on a Buchner funnel, washed with water and dried in air at RT. The synthesized solid was then calcined at 813 K for 1 h in flowing N_2 (150 cm^3/min), followed by 6 h in flowing air (150 cm^3/min). The solid was characterized by BET, XRD and TGA.

The catalyst precursor was prepared by incipient wetness impregnation of MCM-41 with $Fe(NO_3)_3 \cdot 9H_2O$ aqueous solution, at a high enough concentration to obtain a solid with *ca* 5% w/w of iron.

The sample was dried and subsequently calcined in dry N_2 stream (60 cm^3/min) from 298 to 598 K at a heating rate of 0.2 K/min and kept at 598 K for 1 h. The precursor was characterized by atomic absorption spectroscopy, BET, XRD and Mössbauer spectroscopy at 298 and 30 K.

The precursor was reduced in H_2 stream (120 cm^3/min) from 298 to 698 K at 0.28 K/min and kept at 698 K for 26 h. This solid was characterized by CO chemisorption, volumetric oxidation [2], and *in situ* Mössbauer spectroscopy at 298 and 15 K.

Measurements of activity and selectivity were carried out in a fixed bed reactor at 543 K, H_2 : CO ratio of 2 : 1, atmospheric pressure, 20 cm^3/min of total volumetric flow and a space rate of 0.14 s^{-1}. The reaction products were analyzed by gas chromatography using FID and a GS-Gas Pro column.

3. Results and discussion

3.1. SOLID CHARACTERIZATION

The X-ray diffraction pattern of the synthesized solid is shown in Figure 1. The observation of peaks which can be indexed on a hexagonal lattice is typical of MCM-41 material [1]. From the *hkl* : 100 peak the distance between the planes of the pore walls was found to be of 39 Å. A surface area of 1084 m^2/g determined by BET and a narrow distribution of pore sizes similar to those reported in the literature for MCM-41 were found. The pore diameter distribution (Figure 2) leads to an average pore diameter of *ca* 29 Å. Considering the X-ray results, a thickness wall of 10 Å was obtained. The TGA of the sample (Figure 3) showed a weight loss in two steps. The first one between 298 and 373 K assigned to the water surface molecules elimination, and the second one between 546 and 923 K corresponding to the irreversible loss of water associated to the sylanol groups.

After impregnation with iron salt and calcination, XRD results showed that the MCM-41 arrangement remained the same, but the surface area of the solid decreased from 1084 to 730 m^2/g and the pore diameter from 29 to 25 Å, as seen in Figure 2. The atomic absorption spectroscopy determination of the iron

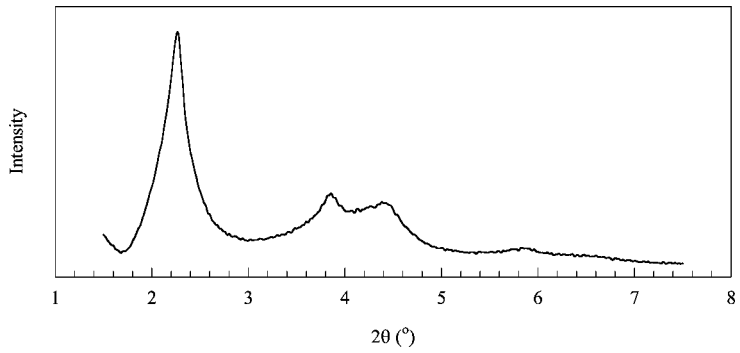

Figure 1. XRD pattern of MCM-41.

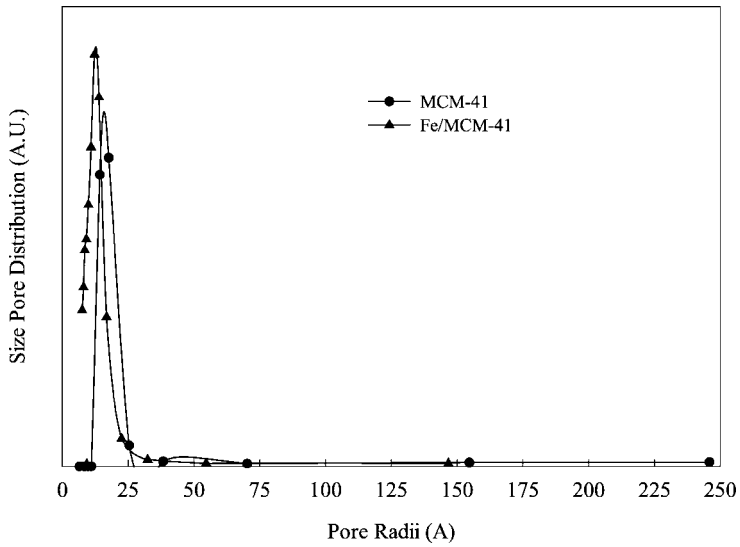

Figure 2. Pore size distribution of MCM-41 and Fe/MCM-41.

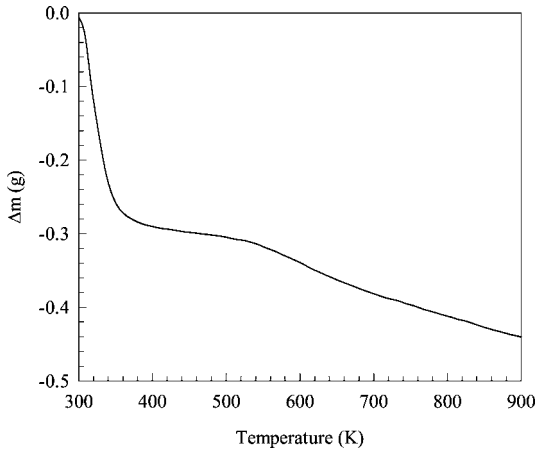

Figure 3. Diagram of thermo-gravimetric analysis of MCM-41.

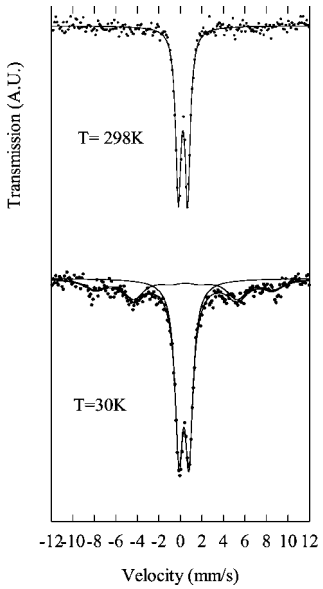

Figure 4. Mössbauer spectra of Fe/MCM-41 precursor at 298 and 30 K.

loading of the precursor yielded 5.9% w/w. The Mössbauer spectrum of the precursor (Figure 4) showed one doublet at 298 K. When the temperature decreased to 30 K, the Mössbauer spectrum displayed two signals: a paramagnetic doublet and a weak and broad magnetic sextet. The values of the hyperfine parameters at both temperatures are characteristic of microcrystals of α-Fe_2O_3 and/or paramagnetic Fe^{3+} ions coordinated with Si–O^- groups. These Si–O^- groups would come from the dehydroxilation of the sylanol groups located on the MCM-41 surface, verified by TGA experiments.

The *in situ* Mössbauer spectra of the reduced sample at both temperatures (Figure 5) showed three components: a singlet, a doublet and a magnetic sextet. The hyperfine parameters can be assigned to the presence of superparamagnetic Fe^0 (Fe^0(sp)) [3, 4], Fe^{2+} [5] and magnetic α-Fe^0 (Fe^0(m)). Table I shows the parameters values and the species percentages (assuming equal recoilless fractions). To estimate roughly the average size of the Fe^0(m) crystals we applied the Collective Magnetic Excitation Model [6] assuming that all the magnetic hyperfine field diminution is due to the very small crystallite size [7]. The diameter estimated in this way was about 173 Å. Taking into account the percentage of Fe^0(m) yielded by Mössbauer spectroscopy and assuming spherical particles of 173 Å diameter, it was possible to calculate a theoretical CO uptake of 2 μmol/g cat. assuming a stoichiometry $Fe : CO = 2 : 1$. We have already mentioned [2] that in amorphous silica Fe^{2+} ions do not chemisorb CO. Therefore, because MCM-41 is made up of amorphous silica walls, the CO consumption by the Fe^0(sp) fraction can be obtained subtracting the CO uptake of Fe^0(m) from the experimental one (Table II). The average diameter calculated, assuming spherical shape and equal

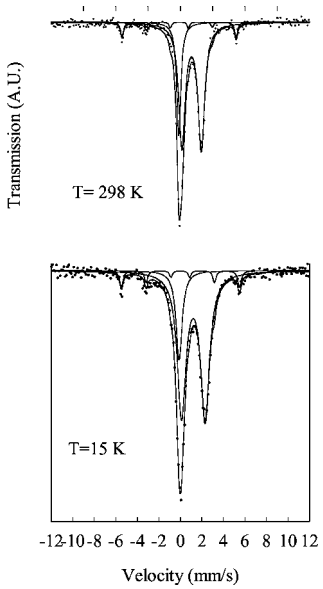

Figure 5. Mössbauer spectra of reduced Fe/MCM-41 at 298 and 15 K.

Table I. Mössbauer hyperfine parameters of the reduced Fe/MCM-41

Temp.	Species	Relative area (%)	Parameters	Fe/MCM-41
298 K	Fe^0(m)	6 ± 1	H (T)	32.9 ± 0.2
			δ (mm/s)	0.00 ± 0.02
			2ε (mm/s)	-0.02 ± 0.04
	Fe^0(sp)	25 ± 4	δ (mm/s)	-0.02 ± 0.01
	Fe^{2+}	68 ± 6	Δ (mm/s)	1.78 ± 0.03
			δ (mm/s)	1.17 ± 0.01
15 K	Fe^0(m)	8 ± 1	H (T)	34.0 ± 0.2
			δ (mm/s)	0.11 ± 0.02
			2ε (mm/s)	0.03 ± 0.05
	Fe^0(sp)	17 ± 1	δ (mm/s)	-0.01 ± 0.01
	Fe^{2+}	75 ± 1	Δ (mm/s)	2.18 ± 0.01
			δ (mm/s)	1.32 ± 0.01

Fe^0(m): magnetic Fe^0.
Fe^0(sp): superparamagnetic Fe^0.

size for all particles of this fraction is 13 Å. Considering the dimensions of the regular arrangement of the support, the Fe^0(m) fraction must be located outside the channels and the Fe^0(sp) fraction would be placed inside them, bearing in mind the diminution of the pore size after impregnation and calcination (Figure 2). The high

Table II. CO chemisorption and volumetric oxidation results

Sample	Fe/MCM-41
CO chemisorption (μmol CO/g)	75 ± 4
D_{VA} (Å)	13
Theoretical volumetric oxidation (μmol O_2/g)	394 ± 12
Experimental volumetric oxidation (μmol O_2/g)	353 ± 18

D_{VA}: average volumetric-superficial diameter.

Table III. Activity and selectivity tests in the Fischer–Tropsch synthesis

	Time (min)		
	66	1385	2474
HC production (molec/g.s) 10^{-17}	12.3	6.4	4.6
Olefins/paraffins	0.096	0.176	0.186
CH_4 (%)	83	82	85
Conversion (%)	14.3	7.8	5.4
Schultz–Flory coefficient (α)	0.187	0.159	0.150

Reaction conditions: 543 K, 1 atm, $H_2 : CO = 2 : 1$ in a fixed bed reactor, using a mass catalyst of 460 mg and a space rate of 0.14 s^{-1}.
HC: hydrocarbon from C_1 to C_5.
α: probability of hydrocarbon chain growth ($0 \leqslant \alpha \leqslant 1$).

content of Fe^{2+} (Table I) indicates a strong iron-support interaction originated by the $(Si–O^-)_2–Fe^{2+}$ coordination. This species would come from the reduction of the paramagnetic Fe^{3+} ions present in the precursor.

The experimental O_2 uptake necessary for the complete reoxidation of the reduced sample is shown in Table II. There is a good agreement between this value and the theoretical O_2 consumption calculated from the percentages of each species obtained from Mössbauer spectrum at 15 K assuming equal f-factors for all iron species. The cross-checking of volumetric oxidation results with Mössbauer spectroscopy is the only reliable method [8] to verify the Mössbauer species assignments.

3.2. ACTIVITY AND SELECTIVITY TESTS

Table III shows the activity and selectivity results at different reaction times for Fe/MCM-41 in Fischer–Tropsch reaction. The hydrocarbon distribution is displayed in the histogram of Figure 6. Since the Fe^0(sp) fraction carries 97% of the total active sites (calculated from the CO uptake of the Fe^0(m) and Fe^0(sp)) the activity and selectivity results will be analyzed in connection with the Fe^0(sp) fraction.

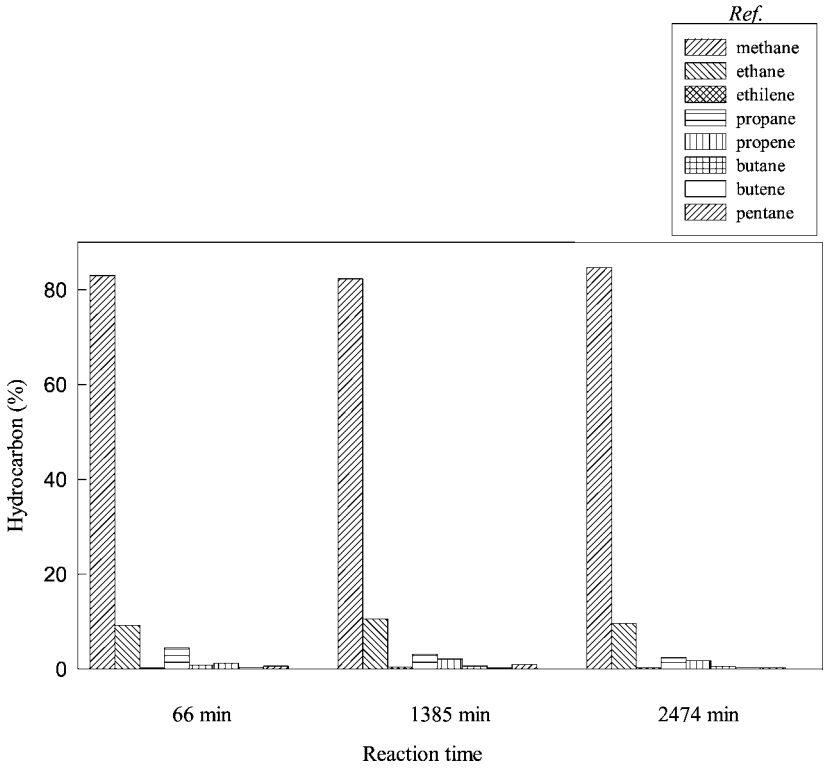

Figure 6. Selectivity histogram in the Fischer–Tropsch reaction of Fe/MCM-41 catalyst at three different times.

Comparing Fe/MCM-41 to a good traditional catalyst for this reaction, like Fe/SiO_2 [9] at similar reaction conditions, it can be seen that the former presents a CO conversion of about six times higher than the latter (7.8% *vs* 1.4%, respectively). Fe/MCM-41 showed a high methane production, which can be justified taking into account that on small metallic particles the hydrocarbon chain growth finishes at low molecular weigh products, obtaining compounds up to C_4 [10]. Although there are no steric constraints inside the pore structure, the very small metallic crystallite size does not allow enough CH_x neighbors to sustain the chain growth. Besides, when the iron crystal size decreases, the activation energy and the amount of weakly chemisorbed hydrogen increases [11]. The high methane production is also due to this fact which leads to a predominance of the termination reaction over the chain growth. This last feature would also be responsible for the low olefin-to-paraffin ratio.

To improve the selectivity towards higher hydrocarbons, experiments are in progress to control the size of the iron crystals inside the channels. Besides, the exchange of the support with alkaline cations will lead to an increase of the olefin production.

4. Conclusions

We have been able to disperse very small crystals of α-Fe_2O_3 inside the channels of a MCM-41 with about 29 Å of pore diameter synthesized in our laboratory. The reduced solid has 24% of Fe^0 and 76% of Fe^{2+}. About 71% of the total Fe^0 crystals – with an average particle size of *ca* 13 Å – are located inside the MCM-41 channels. Probably, the remaining Fe^{2+} ions found in the reduced solid are coordinated to the $Si–O^-$ groups arising from the dehydroxilation of the several hydroxyl groups in the walls of the pores.

Fe/MCM-41 is a very active catalyst for the Fischer–Tropsch reaction, with a high methane production. The high C_1 selectivity may be linked to the very small size of the metallic crystals that cannot sustain the chain growth although the pores are big enough not to impose steric constraints.

Acknowledgements

This work has been partially supported by Consejo Nacional de Investigaciones Científicas y Técnicas (CONICET) (PIP 4326), ANPCyT (PICT 4315), Comisión de Investigaciones Científicas Pcia. Bs. As. (CICPBA) and Universidad Nacional de La Plata, Argentina. The authors thank Ms. Ximena Gonzalez Oddera for her contribution.

S.G.M., M.V.C., N.G.G., R.C.M. and A.A.Y. are members of Carrera del Investigador Científico y Tecnológico, CONICET. A.M.A. and J.F.B. are members of Carrera del Personal del Apoyo, CONICET and CIC, respectively.

References

1. Beck, J. S., Vartuli, J. C., Roth, W. J., Leonowicz, M. E., Kresge, C. T., Schmitt, K. D., Chu, C. T-W., Olson, D. H., Sheppard, E. W., Mc Cullen, S. B., Higgins, J. B. and Schlenker, J. L., *J. Am. Chem. Soc.* **114** (1992), 10 834.
2. Alvarez, A. M., Marchetti, S. G., Cagnoli, M. V., Bengoa, J. F., Mercader, R. C. and Yeramián, A. A., *Appl. Surf. Sci.* **165** (2000), 100.
3. Bødker, F., Mørup, S., Oxborrow, C. A., Linderoth, S., Madsen, M. B. and Niemantsverdriet, J. W., *J. Phys. Cond. Matt.* **4** (1992), 6555.
4. Niemantsverdriet, J. W., van der Kraan, A. M., Delgass, W. N. and Vannice, M. A., *J. Phys. Chem.* **89** (1985), 67.
5. Clausen, B. S. and Topsøe, H., *Appl. Catal.* **48** (1989), 327.
6. Mørup, S. and Topsøe, H., *Appl. Phys.* **11** (1976), 63.
7. Bødker, F., Mørup, S. and Niemantsverdriet, J. W., *Catal. Lett.* **13** (1992), 195.
8. Marchetti, S. G., Cagnoli, M. V., Alvarez, A. M., Bengoa, J. F., Mercader, R. C. and Yeramián, A. A., *Appl. Surf. Sci.* **165** (2000), 91.
9. Gallegos, N. G., Alvarez, A. M., Cagnoli, M. V., Bengoa, J. F., Marchetti, S. G., Mercader, R. C. and Yeramián, A. A., *J. Catal.* **161** (1996), 132.
10. Guczi, L., In: L. Guczi (ed.), *Studies in Surface Science and Catalysis*, Vol. 64, Elsevier, 1991, p. 350.
11. Bartholomew, C. K., In: Z. Paál and P. G. Menon (eds), *Hydrogen Effects in Catalysis. Fundamentals and Practicals Applications*, Vol. 5, Marcel Dekker Inc., 1988, p. 139.